LEATHER SHAVING – A NEW APPROACH FOR UNDERSTANDING THE SHAVING PROCESS

T. Witt[1], E. Klüver[2], A. Nikowski[1] and M. Meyer[2]

1 Technische Universität Dresden, Institut für Naturstofftechnik, 01062 Dresden

2 FILK gGmbH, Meißner Ring 1-5, 09599 Freiberg

a) Corresponding author: tilman.witt@tu-dresden.de

b) Corresponding author: enno.kluever@filkfreiberg.de

Abstract. The shaving process is one of the most important steps in the production of leather, in which an even thickness of the semi-finished product (wet-blue or wet-white) is adjusted by material removal on the rear side. This process is carried out by means of a razor roller in a shaving machine. The success of the shaving process as well as the quality of the resulting surface significantly depend on the long-time experience of the operators. The principles and mechanisms of the underlying cutting process are still insufficiently understood. A current research project deals with the investigation of the cutting process and the interactions between the shaving blade and the material to be processed. The aim is to gain a competent knowledge of the physical processes involved in shaving, which will serve as a basis for the development of new and more effective blades. For this purpose, the theoretical courses of the cutting edge, which describe the expected cut, are to be determined experimentally with the aid of a test setup. The complex cutting behaviour of a knife roller with helical blades will be reduced to a simple model with an exemplary blade. The expected forces can be applied to the cutting edge progressions and their individual determination can be systematized by measurement evaluation. The present study describes the fundamentals of the experimental setup an in addition to that the derivation of a material model for computer simulations.

1 Introduction

The process step of leather shaving involves the removal of material from the rear surface of the flat semi-finished leather product (wet-blue or wet-white) in order to produce a homogeneous thickness. Shaving is performed with the aid of cutting blades arranged helically on a knife roller so the material is removed in the shape of small chips (“leather shavings”). The quality of the shaved leather surface is evaluated, among other things, by the dimensional accuracy of the thickness and the absence of optical artefacts. In general, the shaving process of leather is influenced by the characteristics of the leather, the geometry of the cutting tool and the relative movement of the leather towards the cutting tool. The mechanical properties of the semi-finished leather product are strongly influenced by the preceding manufacturing steps, e.g. liming and tanning. Leather shows viscoelastic properties [1] as well as a highly anisotropic material structure due to its fibrous texture and the locally different orientation and density of the leather fibers [2] [3] [4] [5]. Leather thus differs significantly from metallic or polymeric materials, whose anisotropy is much lower. The geometry of the cutting tools and the guidance of the cut are determined by the given construction of the commercial shaving machines and are limited in their variation possibilities. A key property of cutting processes is a defined cutting edge, which is described in the literature by several approaches concerning natural products. SCHULDT associates the defined cutting edge at the beginning of the cut with an early cut initiation [6], which in turn is affected by the Blade Sharpness Index [7]. A geometric model for material removal can be created under the prerequisite of a defined cutting behaviour. This geometric model is used to apply forces that allow the energy input to be modeled and serves as a fundament for experimental investigations. A test setup based on this model must be able to reduce the cutting behaviour of a knife roll to the cut of a single blade. Furthermore forces and effects occurring during the interaction between blade and leather have to

be determined. From these experimental data, a model for computer simulations will be derived which includes the anisotropy and viscoelasticity of leather and represents a realistic description of the shaving process.

1.1 Approaches on the description of the cutting process

For the separation of materials by cutting, the cutting force can be determined for any point in time. A first distinction in friction and deformation is made according to equation (1) [8] [9].

$$F_{\mathrm{C}} = F_{\mathrm{adhesion}} + F_{\mathrm{deformation}}. \quad (1)$$

Since 1900 there has been a large number of investigations on the cutting of metallic, polymeric and wooden materials. Compared to leather, these materials have a high bending stiffness. In the field of natural materials, the deformation content of the elastic, plastic and viscous area is considered. These properties are also very pronounced in leather, so that a strong similarity is assumed. The term for the deformation is divided into elastic, plastic and viscous [10] contributions, while the adhesion consists of breaking force and friction force [11]. This results in equation (2).

$$F_{\mathrm{C}} = F_{\mathrm{E}} + F_{\mathrm{D,v}} + F_{\mathrm{D,f}} + F_{\mathrm{fract}} + F_{\mathrm{frict}}. \quad (2)$$

F_{E}, $F_{\mathrm{D,v}}$ and $F_{\mathrm{D,f}}$ are the forces that deform the chip, F_{fract} describe the force that separates the material and F_{frict} identifies the friction between the cutting tool and the material. Regarding metallic materials, the plastic deformation of the chip is dominant over the elastic deformation. Based on the work of MERCHANT [8], models were developed to describe and predict the forces occurring during orthogonal cutting [12]. Other models were developed and investigated for the more complex oblique cutting [13] [14] [15]. The cutting of composite materials is even more complex due to the existing anisotropy. In his experiments, KOPLEV [16] showed that the fiber orientation of carbon fibers in an epoxy matrix is decisive for the forces occurring and the progress of the cut. **Fig. 1** shows that in orthogonal fiber orientation no premature cut can be seen, which significantly distinguishes the mechanical processing of composite materials and metals.

Fig. 1. Cross section of 'quick-stop' specimen showing the notch formed by the tool: (a) machined perpendicular the fibers. (b) machined parallel to the fibers. [16]

Further experiments and modelling with different approaches allow better predictions [17] [18]. This shows that the mechanical machining of composite materials poses different challenges than the machining of metals. The approach used so far for these materials is inadequate. The orientation of the fibers in relation to the relative direction of movement of the cutting tool is of particular importance. The investigations with fiber-reinforced plastic from SREEJITH [19] showed that the surface quality is dependent on the fiber orientation and must be taken into account during processing. **Fig. 2** shows the problem of fiber orientation for the shaving process of leather. An undesirable effect when shaving leather is the formation of a staircase-shaped texture, which can probably be explained with similar relationships.

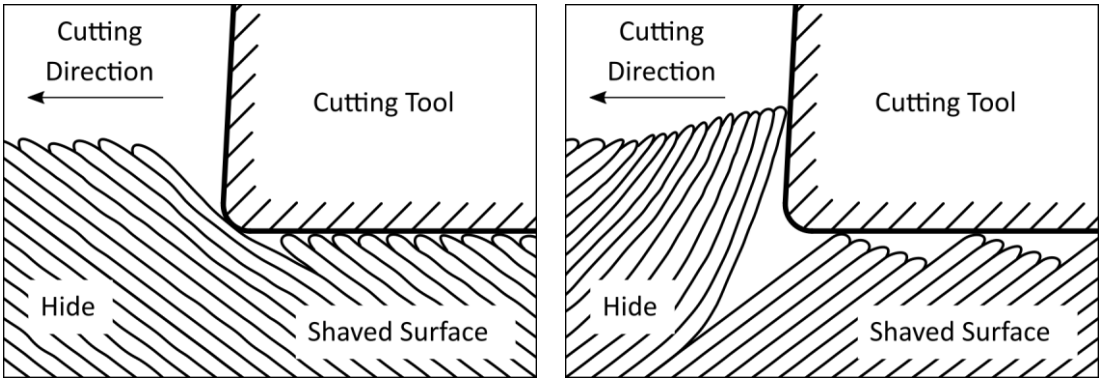

Fig. 2. Shaving under consideration of the fiber alignment.

In addition, SREEJITH's study found that with increasing cutting speed, both cutting force and cutting temperature do not increase uniformly and there is a local minimum. Increasing the feed rate, on the other hand, leads to a lower feed force and a higher temperature. CALZADA [20] presented a fracture model for fibers in which different types of fracture could be detected depending on the fiber orientation. The modelling of composite materials with fibers is still part of current research [21] [22] [23]. The approach functions for modelling refer to geometric predictions for chip formation. The work of BUSHLYA [24] provides a summary of the geometric determination of cutting volumes and cutting lengths for milling work.

1.2 Shaving Process

Leather shaving machines are an integral part of a tannery and have been used in their basic design since the end of the 19th century [25]. Their function is to produce a certain thickness of a flexible surface material by chip removal. For this purpose, the flexible semi-finished leather product is guided over a chrome-plated roller. On a second roller, the helix-shaped blades are arranged symmetrically with reference to the center. The gap between the rollers determines the thickness of the product after the process. The principle arrangement of the rollers and the directions of movement are shown in **Fig. 3**.

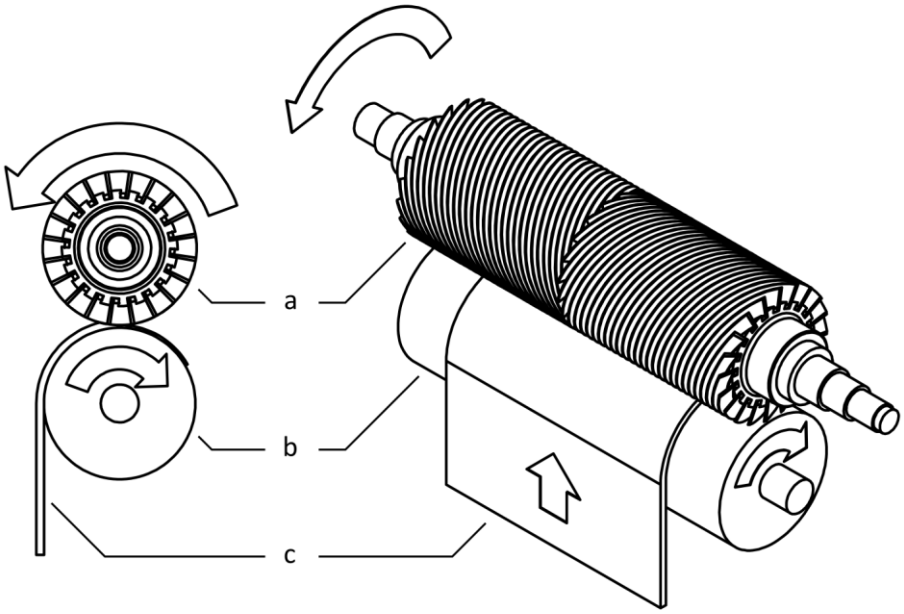

Fig. 3. Active unit for the shaving of leather with moving direction indicators. (a) Knife roller. (b) Chrome-plated roller. (c) Leather.

The blades are continuously sharpened with a grinding wheel in order to achieve a constantly high sharpness. Due to the different sizes of different animals, machines are available in various working widths. In addition, there are differences in the cylinder diameter of the chrome and knife roller as well as different pitches of the blades. The pitch angle of the knife roller λ_{Kr} plays an important role in this investigation and is calculated according to equation (3) from the pitch of the spiral per revolution P_{Kr} and the diameter of the blade shaft d_{Kr}.

$$\lambda_{\mathrm{Kr}} = \arctan\left(\frac{P_{\mathrm{Kr}}}{\pi \cdot d_{\mathrm{Kr}}}\right) \cdot \frac{180^\circ}{\pi}. \tag{3}$$

Fig. 4 is derived on the basis of collected machine data. It shows the pitch of the blades in respect to different core diameters of the knife roller. The data set includes the blades from two different manufacturers.

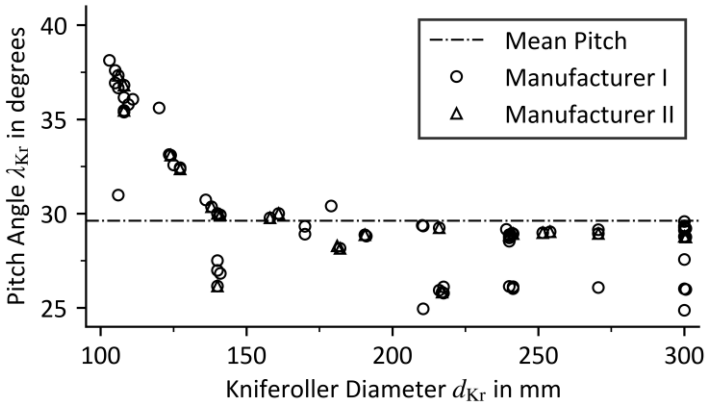

Fig. 4. Pitch angle of the knife roller in respect to different core diameters of the knife roller from two different manufacturers and the mean value of the pitch.

The pitch angle of the knife roller λ_{Kr} of slightly less than 30° is dominant and corresponds approximately to the mean value of the data set. Due to the pitch of the helix, the orientation of the cutting edge is not orthogonal to the current feed direction. This results in an oblique cut. The feed rate is set or indicated on the machine in meters per minute and the speed of the measuring cylinder is specified in revolutions per minute (rpm).

2 Material and Methods

2.1 Exemplary machine data

For the analysis of the shaving process the machine Arenco-BMD type FM 1800 is used as an example. The machine has a working width of 1800 mm. The cutting tool rotates at a speed of 1500 rpm and has a knife roller diameter of 252 mm, which is reduced by grinding. The lower limit of the blade length is assumed to be 10 mm. The pitch of the knife helix is 330 mm per revolution and thus has a pitch angle of about 30 degrees. The chrome-plated roller has a measured radius of 92 mm. A feed rate of 6 m/min to 21 m/min can be set. The number of blades varies depending on the machine version with 9, 12, 15 or 18 pieces. A number of blades of 15 is assumed for further consideration.

2.2 Calculation of characteristic geometric quantities

To determine the basic geometric properties of a cut, the length of the cutting edge, the theoretical maximum thickness of the chip and the displaced area per cutting operation are used. The calculation of these values from metal processing is adapted for the feed movement on a circular path to represent the process of leather shaving. The variables relevant for the calculation are shown in the schematic sketch (**Fig. 5**).

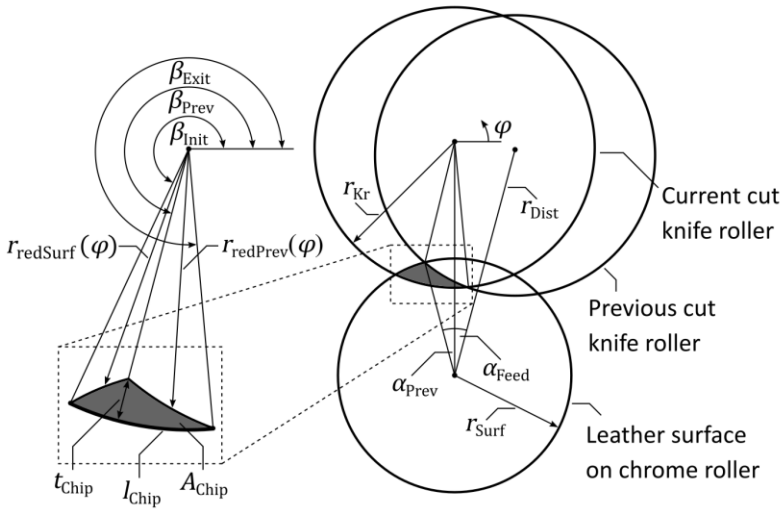

Fig. 5. Schematic sketch of the geometric structure with the relevant variables.

The radius of the surface of the leather is determined by the diameter of the chrome roller d_{Cr} and the thickness of the leather t_H.

$$r_{Surf} = \frac{d_{Cr}}{2} + t_H. \tag{4}$$

The initial contact of the cutting tool with the leather surface is described by the angle β_{Init}, which is calculated according to the cosine theorem from the triangle of the surface radius r_{Surf}, the distance of the pivot points of the knife roller and chromium roller r_{Dist} and the radius of the knife roller r_{Kr}.

$$\beta_{Init} = \frac{3 \cdot \pi}{2} - \arccos\left(\frac{r_{Dist}^2 + r_{Kr}^2 - r_{Surf}^2}{2 \cdot r_{Dist} \cdot r_{Kr}}\right). \tag{5}$$

The feed angle α_{Feed} is required to calculate the exit angle β_{Exit}. For reasons of clarity, the last section of a spiral is also shown as a circle in **Fig. 5**. The feed angle can be calculated from the feed speed of the leather v_{Feed}, the rotation speed of the knife roller n_{Kr}, the number of blades on the knife roller i_K and the radius of the surface r_{Surf}.

$$\alpha_{Feed} = \frac{v_{Feed}}{n_{Kr} \cdot i_K \cdot r_{Surf}}. \tag{6}$$

The exit angle β_{Exit} at the point of exit of the helix is to be determined by the intersection of the circles of the current cut and the previous cut. Two mathematical angles result from the solution of the equation. Due to the given arrangement, the smaller angle is to be used.

$$\beta_{Exit} = \frac{3 \cdot \pi}{2} + \arcsin\left(\frac{r_{Dist}}{r_{Kr}} \cdot \sin\frac{\alpha_{Feed}}{2}\right) - \frac{\alpha_{Feed}}{2}. \tag{7}$$

The upper and lower limits of the polar index variable φ are thus present. With the knife radius r_{Kr} and the limits of the angle φ the curve $\gamma(\varphi)$ for the cutting edge is set up. The pitch in axial direction per revolution p_{Kr} is added in the third spatial direction and set depending on φ.

$$\gamma_{\mathrm{Edge}}(\varphi) = \begin{pmatrix} r_{\mathrm{Kr}} \cdot \cos\varphi \\ r_{\mathrm{Kr}} \cdot \sin\varphi \\ \frac{p_{\mathrm{Kr}}}{2\cdot\pi} \cdot \varphi \end{pmatrix}, \quad \beta_{\mathrm{Init}} \leq \varphi \leq \beta_{\mathrm{Exit}}. \tag{8}$$

The derivation of the curve according to the index variable φ is necessary for the application in the curve integral.

$$\gamma'_{\mathrm{Edge}}(\varphi) = \begin{pmatrix} -r_{\mathrm{Kr}} \cdot \sin\varphi \\ r_{\mathrm{Kr}} \cdot \cos\varphi \\ \frac{p_{\mathrm{Kr}}}{2\cdot\pi} \end{pmatrix}, \beta_{\mathrm{Init}} \leq \varphi \leq \beta_{\mathrm{Exit}}\,. \tag{9}$$

The length of the cutting edge is formulated with a curve integral, which is formed according to the rule in equation (10).

$$l_{\mathrm{Chip}} = \int_{\beta_{\mathrm{Init}}}^{\beta_{\mathrm{Exit}}} \left\| \gamma'_{\mathrm{Edge}}(\varphi) \right\| \mathrm{d}\varphi. \tag{10}$$

The radii of the edges of the knife roller and leather upper edge must be determined as a function of the index variable φ in order to determine the thickness of the chips and the displaced area. This requires a further integration limit. The upper edge of the chip is partly determined by the surface of the uncut leather and partly by the previous cut. In a first step, the angle of the preceding cut α_{Prev} is determined in relation to the axis of rotation of the chrome roller.

$$\alpha_{\mathrm{Prev}} = \arccos\left(\frac{{r_{\mathrm{Surf}}}^2 + {r_{\mathrm{Dist}}}^2 - {r_{\mathrm{Kr}}}^2}{2 \cdot r_{\mathrm{Surf}} \cdot r_{\mathrm{Dist}}}\right) \tag{11}$$

The angle α_{Prev} determines the angle β_{Prev} for the coordinate system of the current cutter roller.

$$\beta_{\mathrm{Prev}} = \frac{3\cdot\pi}{2} + \arctan\left(\frac{\sin(\alpha_{\mathrm{Prev}} - \alpha_{\mathrm{Feed}}) \cdot r_{\mathrm{Surf}}}{r_{\mathrm{Dist}} - \cos(\alpha_{\mathrm{Prev}} - \alpha_{\mathrm{Feed}}) \cdot r_{\mathrm{Surf}}}\right). \tag{12}$$

The first part of the surface has not yet been cut. There are two solutions, whereby in the given arrangement the radius with the smaller amount must be used.

$$r_{\mathrm{redSurf}}(\varphi) = \sin(-\varphi) \cdot r_{\mathrm{Dist}} \pm \sqrt{(\sin^2(-\varphi) - 1) \cdot {r_{\mathrm{Dist}}}^2 + {r_{\mathrm{Surf}}}^2}, \quad \beta_{\mathrm{Init}} \leq \varphi \leq \beta_{\mathrm{Prev}}. \tag{13}$$

The maximum thickness of the chip t_{Cut} is determined using the reduced radius $r_{redSurf}(\varphi)$ at the location of the β_{Prev} angle.

$$t_{\mathrm{Chip}} = r_{\mathrm{Kr}} - r_{\mathrm{redSurf}}(\beta_{\mathrm{Prev}}). \tag{14}$$

The second part of the upper edge is determined by the previous cut. The variable radius $r_{redPrev}(\varphi)$ describes the upper edge within the limits β_{Prev} to β_{Exit}. The solution of the square equation gives two results. The root term must be added for the given arrangement.

$$r_{\mathrm{redPrev}}(\varphi) = \pm\sqrt{4 \cdot {r_{\mathrm{Dist}}}^2 \cdot \sin^2\left(\frac{\alpha_{\mathrm{Feed}}}{2}\right) \cdot \cos^2\left(\varphi + \frac{\alpha_{\mathrm{Feed}}}{2}\right) + {r_{\mathrm{Kr}}}^2}, \quad \begin{matrix} 2r_{\mathrm{Dist}} \sin\frac{\alpha_{\mathrm{Feed}}}{2} \cdot \cos\left(\varphi + \frac{\alpha_{\mathrm{Feed}}}{2}\right) \\ \beta_{\mathrm{Prev}} \leq \varphi \leq \beta_{\mathrm{Exit}}. \end{matrix} \tag{15}$$

In a final step, the formulation of the area integral for the displaced area A_{Chip} is given in the form of a double integral.

$$A_{\mathrm{Chip}} = \begin{matrix} \int_{\beta_{\mathrm{Init}}}^{\beta_{\mathrm{Exit}}} \int_0^{r_{\mathrm{Kr}}} \sqrt{\left(\frac{p_{\mathrm{Kr}}}{2 \cdot \pi}\right)^2 + r^2}\, \mathrm{d}r\, \mathrm{d}\varphi \\ - \int_{\beta_{\mathrm{Init}}}^{\beta_{\mathrm{Prev}}} \int_0^{r_{\mathrm{redSurf}}(\varphi)} \sqrt{\left(\frac{p_{\mathrm{Kr}}}{2 \cdot \pi}\right)^2 + r^2}\, \mathrm{d}r\, \mathrm{d}\varphi \cdot \\ - \int_{\beta_{\mathrm{Prev}}}^{\beta_{\mathrm{Exit}}} \int_0^{r_{\mathrm{redPrev}}(\varphi)} \sqrt{\left(\frac{p_{\mathrm{Kr}}}{2 \cdot \pi}\right)^2 + r^2}\, \mathrm{d}r\, \mathrm{d}\varphi \end{matrix} \tag{16}$$

With equations (10), (14) and (16), the three characteristic quantities of the cutting process can be calculated and used for sensitivity analyses.

2.3 Determination of the torque based on the rotational speed for an electric motor

The determination of the prevailing load in a processing operation can be determined on the basis of the load acting on the driving motor. In the FM 1800 shaving machine, the knife roller and the scraper roller are driven by a 225M three-phase motor with 45 kW and 1500 rpm. A motor of the same design was procured and tested on a test stand to determine the torque as a function of the speed of rotation of the motor. The test stand is presented in detail in the dissertation by WINDISCH [26]. The test arrangement is shown in **Fig. 6**.

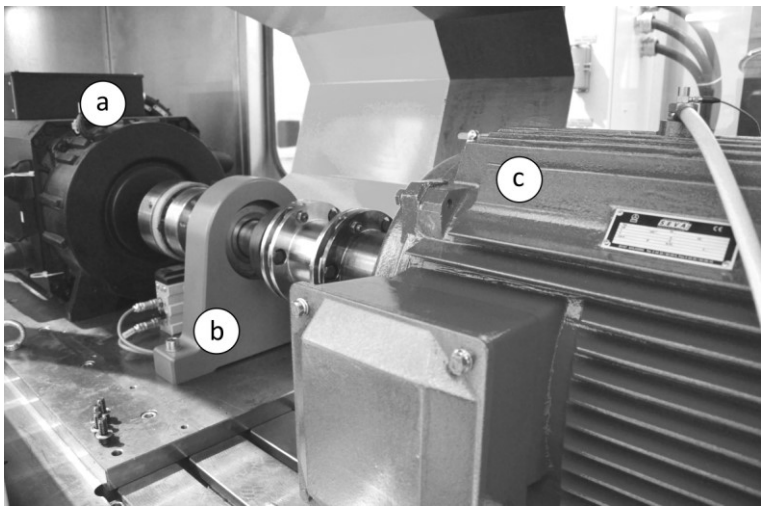

Fig. 6. Test arrangement for torque determination. (a) Brake motor. (b) Torque sensor. (c) Engine under test.

On the bench, the brake motor (a) is connected to the torque sensor (b) by a coupling and the latter is connected to the motor (c) to be tested by another coupling. The motor runs under rated load for 20 minutes to allow the motor to reach operating temperature. The test series is operated with a software which sets a speed at the dominant brake motor and holds it for 10 seconds. The measured torque values are recorded over the period for the rotational speed. Finally, the torque curve is approximated by a linear regression in respect to the rotational speed.

3 Results

3.1 Sensitivity analysis for a type FM 1800 machine

The sensitivity analysis is performed for a machine Arenco-BMD type FM 1800 with different parameter variations. On the machine, settings can be realised with regard to the feed speed, the shaving gap and the speed of the blade roller by means of a frequency converter added subsequently. On the material side, the process is influenced by the initial thickness of the leather and the target thickness. For the calculation, it is assumed that the thickness after shaving corresponds exactly to the width of the gap. The calculation always assumes a thickness of 4 mm to be manufactured, whereby the initial thickness of the leather is varied from 4.1 to 4.8 mm, which consequently corresponds to a removed height of 0.1 to 0.8 mm. The influence of the removal and the machine parameters (motor turning speed n_{Motor}, diameter of the cutting cylinder r_{Kr} and feed rate v_{Feed}) are graphically shown in **Fig. 7**, **Fig. 8** and **Fig. 9**. The cutting depth is plotted on the x-axis, while the y-axis represents one of the three machine parameters. The change in the diameter of the cutting cylinder is a consequence of the grinding of the knives. The range of variation of the parameters is shown in **Table 1**. All other parameters are considered constant.

Table 1. Parameter variations.

Graph	t_{Cut} in mm	n_{Motor} in 1/min	r_{Kr} in mm	v_{Feed} in m/min
I	0.1 - 0.8	1200 - 1800	115	12
II	0.1 - 0.8	1500	105 - 125	12
III	0.1 - 0.8	1500	115	8 - 16

The results of the sensitivity analysis are displayed graphically as a surface plot. First of all, the influence of the engine speed and the removal height are examined in **Fig. 7**.

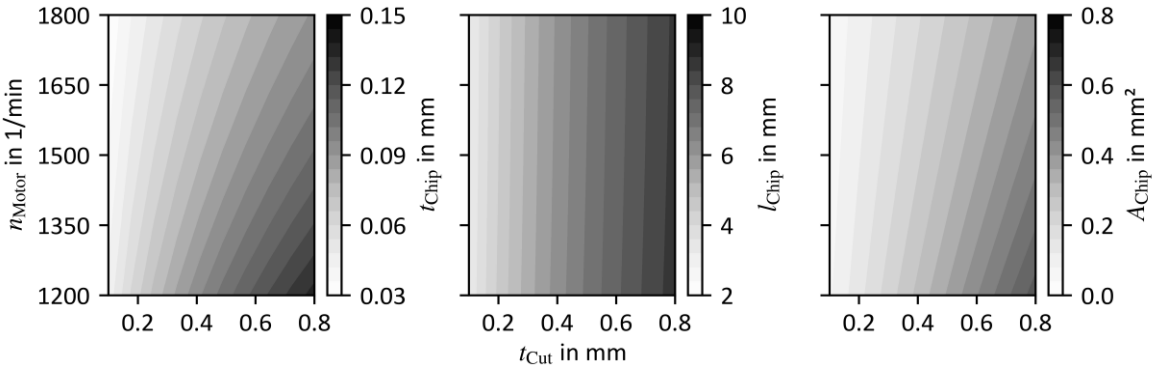

Fig. 7. Response variables as a function of cutting depth and engine speed.

The change in the rotational speed of the motor (**Fig. 7**) has a minor influence on the cutting edge length. Both the maximum thickness of the chip and the cross-sectional area of the chip decrease with increasing speed of the motor.

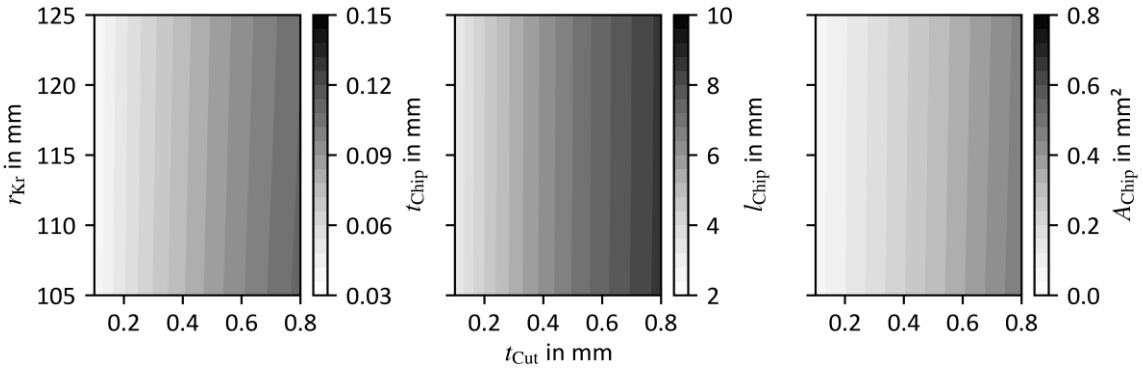

Fig. 8. Response variables as a function of cutting depth and knife roll diameter.

The change in the diameter of the knife roller (**Fig. 8**) has very little effect on the quality criteria for the area investigated. A tendency can be seen, but this is hardly noticeable with a knife roller diameter of 200 mm or more.

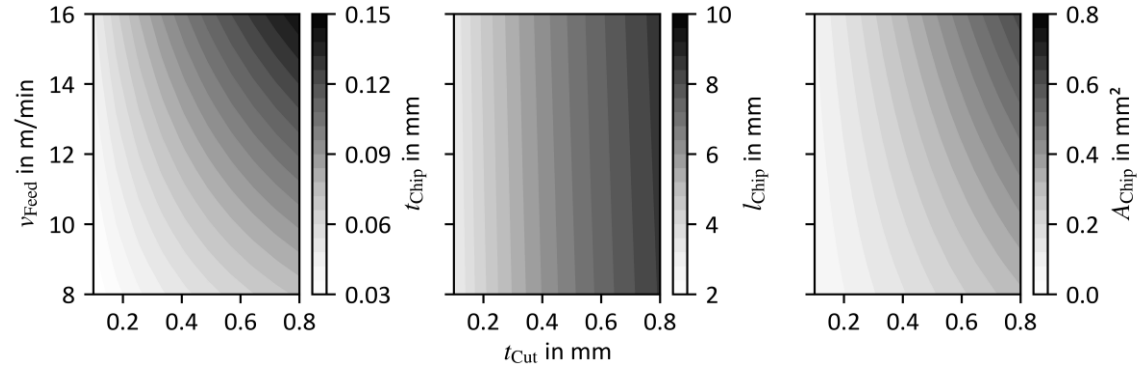

Fig. 9. Response variables depending on cutting depth and feed rate

An increase in the feed rate (**Fig. 9**) results in an increase in the thickness of the chip. The increase is reinforced nonlinearly by an increase in the cutting depth. As in the previous cases, the length of the cutting edge is only slightly influenced by the feed rate. The displaced area increases in a similar way due to the increase in chip thickness.

3.2 Torque characteristics for the main drive of a machine of type FM 1800

The tests to determine the torque curve as a function of the rotational speed were carried out with a new motor of size 225M with an output of 45 kW and 1500 rpm. The results of the tests are shown in **Fig. 10**.

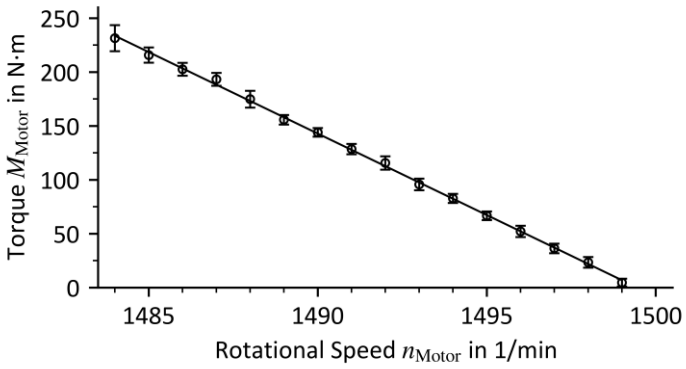

Fig. 10. Motor torque in respect to rotational speed. The linear regression applies to the test points with standard deviation.

The equation (17) for linear regression does not lead through the idle speed of 1500. This is due to fluctuations in the electrical grid.

$$M_{\mathrm{Motor}}(n_{\mathrm{Motor}}) = -15.121 \cdot n_{\mathrm{Motor}} + 22673\ . \qquad (17)$$

This enables to determine the mechanical load in the process by specifying the torque for the turning frequency in the range of 1485 to 1500 rpm.

3.3 Torque during shaving of cattle hides

The tests were carried out on a machine Arenco-BMD type FM 1800 with half hides of cattle. The machine was additionally equipped with a rotary position sensor. The process load is determined from the encoder data and the determined relationship between torque and rotational speed. The machine has 15 helical blades on both sides and was operated with a feed speed of 9 m/min. The skins were tanned with glutaraldehyde and the thickness was measured before and after shaving. The gap between chrome roller and knife roller was set to 0.8 mm. The shaved hides had a thickness of 1.1±0.2 mm. Each individual leather was first shaved from the tail two thirds. Then the leather was removed from the machine, turned and the remaining third of the skin was treated. The experiments were carried out with hides. **Fig. 11** shows the motor torque M_{Motor} curves for the first side on the left and the 6 torque curves for the second side for the shaving process on the right.

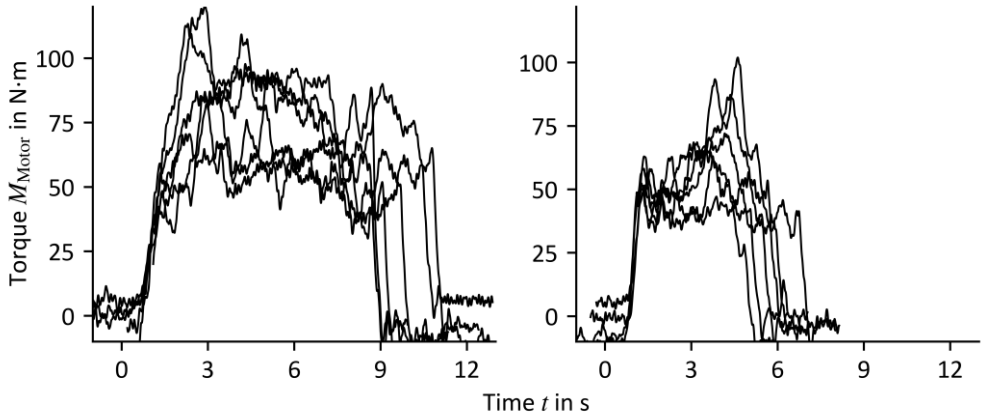

Fig. 11. Motor torque in respect to time during shaving. Process starting from the tail (left). Process starting from the neck (right).

The curves are post-synchronized in **Fig. 11** to obtain a comparable representation. The mean value from the torque curve is determined for shaving on the tail side M_{Tail} and on the head side M_{Head} for the time range t = 1.5 s to t = 4.5 s for each curve. The torques as well as the maximum and minimum thickness t_{min} and t_{max} for the hides are documented in **Table 2**.

Table 2. Thickness of cattle hides before shaving.

Hide	I	II	III	VI	V	VI
t_{Min} in mm	1.5	1.3	1.6	1.6	1.4	1.4
t_{Max} in mm	1.7	1.5	1.8	1.8	1.6	1.6
M_{Tail} in N · m	93.7	59.7	76.8	59.8	66.3	87.6
M_{Neck} in N · m	53.4	40.7	59.2	59.8	43.8	54.0

Although the initial thicknesses are relatively similar, a strong divergence of the measured values can be observed. This is due, among other things, to the different widths of the hides and the

general inhomogeneity of the natural material. The mean value of all torques is 62.9 N with a standard deviation of 16.0 N. No further statistical evaluation is carried out due to the small number of hides examined and the low variance of the setting parameters.

4 Discussion

Based on the results, it can be assumed that the length of the active cutting edge cannot be influenced to any relevant extent by variations in the machine settings. All investigated parameters, on the other hand, show a very strong influence on the thickness of the removed chip. MERCHANT already held that the mechanical work caused by forming accounts for a large proportion of the cutting work. On the other hand, the investigations by SREEJITH and CALZADA show that the fiber orientation is of great importance for the proportion of deformation work to cutting work. The material to be processed is markedly viscoelastic. With a constant chip thickness and a higher processing speed it is expected that a considerably higher deformation work is to be performed. This is in line with practical experience, according to which the rotational speed of the motors decreases more as the thickness of the leather to be shaved increases. The measurements of the torque when shaving cattle hides give a first indication of the forces to be expected during the shaving process. However, the number of tests must be increased considerably in order to be able to make reliable statements. In particular, the differences due to moisture and the tanning process must be investigated more extensively in order to provide a stable data basis for the simulation. Nevertheless, the created data are sufficient to serve as a reference for the comparison with first simulations.

5 Conclusions

The shaving of leather is comparable to the cutting of composite materials and therefore the findings in this field can serve as a basic principle for the onward development of the shaving process. The settings on the leather shaving machines plus the modification options of the cutting geometry provide the basis for an experimental investigation on the shaving process. The execution of designed tests combined with the developed geometric correlations will determine the most important parameters influencing the shaving process. Initial tests have been used to determine the essential values that will allow simulation results to be checked. An optimized geometry of the cutting tools has to be determined by using a computer simulation of the cutting process.

Acknowledgements

We gratefully acknowledge the German Federal Ministry for Economic Affairs and Energy for financial support within the Central Innovation Program for small and medium-sized enterprises (ZIM). We are grateful to Heusch GmbH for their participation in the project and to SÜDLEDER GmbH for their support in large-scale experiments. Stefan Gütling is acknowledged for the preparation of leather samples and the performance of shaving experiments.

References

1. *Ward, A. G.: The mechanical properties of leather, Rheologica Acta, 12, pp. 103-112, 1974*
2. *Haines, B.M.: Review. The Anatomy of Leather, Journal of Materials Science, 10, pp. 528-538, 1975*
3. *Michel, A.: Variations within hides and skins. Part 1: The Influence of the Fibre Structure, World Leather, Nr. October/November, pp. 18-19, 2009*
4. *Basil-Jones, M. M.: Collagen Fibril Orientation in Ovine and Bovine Leather Affects Strength: A Small Angle X-ray Scattering (SAXS) Study, Journal of Agricultural and Food Chemistry, 59, pp. 9972-9979, 2011*
5. *Basil-Jones, M. M.: Collagen Fibril Orientation and Tear Strength across Ovine Skins, Journal of Agricultural and Food Chemistry, Journal of Agricultural and Food Chemistry, 61, pp. 12327-12332, 2013*
6. *Schuldt, S.: High-speed cutting of foods: Cutting behavior and initial cutting forces, 230, pp. 55-62, 2018*
7. *McCarthy, C. T.: On the sharpness of straight edge blades in cutting soft solids: Part II–Analysis of blade geometry, Engineering Fracture Mechanics, 77, pp. 437-451, 2010*
8. *Merchant, M.: Mechanics of the metal cutting process. I. Orthogonal cutting and a type 2 chip, Journal of applied physics, 16, pp. 267-275, 1945*
9. *Bowden, F.: Friction, lubrication and wear: a survey of work during the last decade, British Journal of Applied Physics, 12, p. 1521, 1966*
10. *Van Vliet, T.: Large deformation and fracture behaviour of gels, Current Opinion in Colloid & Interface Science, 1, pp. 740-745*
11. *Atkins, A. G.: Fracture toughness and cutting, International Journal of Production Research, 12, 263-274, 1974*
12. *Budak, E.: Prediction of milling force coefficients from orthogonal cutting data, Journal of Manufacturing Science and Engineering, 118, pp. 216-224, 1996*
13. *Moufki, A.: Thermoviscoplastic modelling of oblique cutting: forces and chip flow predictions, International Journal of Mechanical Sciences, 6, pp. 1205-1232, 2000*
14. *Li, S. J.: Dynamic force modelling for a ball-end milling cutter based on the merchant oblique cutting theory, The International Journal of Advanced Manufacturing Technology, 7, pp.477-483,2001*
15. *Moufki, A.: Thermomechanical modelling of oblique cutting and experimental validation, International Journal of Machine Tools and Manufacture, 9, pp.971-989, 2004*
16. *Koplev, A.: The cutting process, chips, and cutting forces in machining CFRP, Composites, 14, pp. 371-376, 1983*
17. *Dandekar, C. R.: Modeling of machining of composite materials: A review, International Journal of Machine tools and manufacture, 57, pp. 102-121, 2012*
18. *Che, D.: Machining of carbon fiber reinforced plastics/polymers: a literature review, Journal of Manufacturing Science and Engineering, 136, pp. 034001, 2014*
19. *Sreejith, P. S.: Evaluation of PCD tool performance during machining of carbon/phenolic ablative composites, Journal of Materials Processing Technology, 104, pp. 53-58, 2000*
20. *Calzada, K.: Modeling and interpretation of fiber orientation-based failure mechanisms in machining of carbon fiber-reinforced polymer composites, Journal of Manufacturing Processes, 14, pp. 141.149, 2012*
21. *Wan, M.: Cutting force modelling in machining of fiber-reinforced polymer matrix composites (PMCs): a review, Composites Part A: Applied Science and Manufacturing, 2018*
22. *Wang, H.: Modeling and analysis of force prediction in milling process of unidirectional fiber reinforced polymer composites, The International Journal of Advanced Manufacturing Technology, pp. 1-8, 2018*
23. *Shang, S.: A bond-based peridynamic modeling of machining of unidirectional carbon fiber reinforced polymer material, The International Journal of Advanced Manufacturing Technology, pp. 1-8, 2018*
24. *Bushlya, V.: On the Analytical Representation of Chip Area and Tool Geometry when Oblique Turning with Round Tools. Part 1: Chip Area Parameters under Variation of Side and Back Rake Angle, Procedia CIRP, 31, pp. 417-422, 2015*
25. *Landmann, W.: The Machines in the Tannery, Dewsbury: World Trades Publishing, 2003*
26. *Windiwsch, T.: Energieeffiziente Antriebsregelung für hochausgenutzte Drehstrommotoren in elektrisch angetriebenen Fahrzeugen, Shaker Verlag, 2018*